

## Global equatorial sea-surface temperatures over the last 150,000 years: an update from foraminiferal elemental analysis

Rajeev Saraswat\*

Micropaleontology Laboratory, Geological Oceanography Division, National Institute of Oceanography, Dona Paula, Goa 403 004, India

Solar insolation changes are amongst various factors that affect sea-surface temperature (SST) which in turn modulate global climate. Out of all the oceanic regions, equatorial region receives the maximum solar insolation and thus is the locale for the warmest waters. However, how the equatorial SST affects global climate, is still not clear. Long-term past seawater temperature records are required to understand the effect of temporal changes in equatorial SST on the global climate. Various techniques are used to estimate past seawater temperatures. Here, the equatorial SSTs of the last 150,000 years BP as estimated from Mg/Ca ratio of the foraminiferal shells, have been compiled in order to get an update of the past SST changes in the equatorial region. It is inferred that the average cooling during the Last Glacial Maximum (LGM) (the interval dated from ~19–23 kyr BP during the last glacial period, when the ice-sheets covered maximum area) was ~2.3°C as compared to the Holocene. The LGM–Holocene SST difference was not uniform throughout the studied cores, which implies that the surface equatorial temperature gradient during LGM was different than that at present. The equatorial surface waters were warmest during marine isotopic stage (MIS) 5.5, even warmer than that at present. However, the pattern of cooling and amount of drop in surface temperature during various sub-stages of MIS 5 was not uniform throughout the equatorial oceans. During MIS 4, several regions of the surface equatorial ocean were warmer than that during MIS 3. The study further shows that surface equatorial oceans during MIS 3 were as cold as during MIS 2.

**Keywords:** Equatorial, foraminifera, glacial, interglacial, Mg/Ca, sea-surface temperature.

THE physico-chemical state (temperature, salinity, pH, etc.) of the oceans modulates the global climate. While high latitude northern and southern polar oceanic regions are the locale for the deepwater formation and thus dissipation of heat, tropical and equatorial oceans contribute the maximum warmth to the global oceans<sup>1</sup>. The equatorial seawater temperature is among several factors that modulate global climate, particularly the monsoons in the Indo-Pacific region<sup>2</sup>. In order to precisely predict the

imminent climatic changes, it is essential to understand the relationship between state of the ocean and the global climate. A comparison of oceanic properties, particularly temperature, reconstructed from marine sediments recovered from different parts of the world oceans, with the climatic variables as inferred from terrestrial records (sediments, tree rings, ice cores, speleothems, etc.), of the time spans covering large climatic variability, helps to assess the ocean's role in global climatic changes. The Quaternary period includes several long glacial intervals, wherein ice sheets increased tremendously, followed by a relatively rapid warming phase which lead to large-scale collapse and melting of ice-sheets (known as deglaciation). Following the deglaciation, warm periods lasted only for a small interval, known as interglacial. Large climatic changes occurred during the last such interglacial and glacial cycles, followed by the present interglacial period (~150 kyr BP). Therefore, extensive efforts are made to generate seawater temperature records covering the last 150 kyr BP.

The first extensive effort to determine global sea-surface temperature (SST) during the Last Glacial Maximum (LGM), the period of maximum ice-sheet extent since the last interglacial, was made as part of the 'Climate: Long range Investigation, Mapping, and Prediction (CLIMAP)' project undertaken in the 1970s and 1980s. The outcome of the CLIMAP project was no or little cooling in the equatorial region during LGM. However, an overall cooling of the earth by  $3.0 \pm 0.6^\circ\text{C}$  during LGM was estimated<sup>3–5</sup>. The occurrence of distinct assemblages of planktic foraminifera in waters of different temperatures was utilized during the CLIMAP project. However, the reliability of CLIMAP-estimated SSTs was questioned, especially because it interpreted warmer western Pacific during LGM<sup>6</sup>. Similar results were obtained as part of early efforts to model temperatures during LGM<sup>7</sup>.

Another important time period to understand the future climatic changes, especially the consequences of global warming, is the last interglacial, the last time when global temperature was supposedly as high as that at present or even more than that at present. It can be used as an analogue of the present interglacial but without anthropogenic influence. The attempt to reconstruct temperatures during the last interglacial (marine isotopic stage 5e), again under the CLIMAP project was marred by no-analogue problem, which refers to the absence of living counterparts of the fossil assemblages<sup>3</sup>. Since the CLIMAP estimates were based on transfer function of the modern distribution of planktic foraminifera in the global oceans, which was based on a limited coverage of samples, later on additional samples were collected from different oceans as part of another global effort termed 'Multiproxy Approach for the Reconstruction of the Glacial Ocean Surface (MARGO)' project, and the transfer functions were modified. It refined estimates of LGM cooling<sup>8</sup>. Meanwhile, other individual studies provided valuable insight

\*e-mail: rsaraswat@nio.org

into the SST changes over the glacial–interglacial periods. Since the transfer function is based on proper identification of foraminiferal species in every sample, it was time-consuming, subjective and had large possibility of errors; even the replication of the data was difficult.

Past seawater temperature has also been estimated by several other techniques including unsaturation indices preserved in sedimentary organic matter<sup>9</sup>, stable oxygen isotopic ratio of planktic foraminifera<sup>4</sup>, Sr/Ca ratio of corals, transfer function of faunal composition<sup>10,11</sup>. In the mid-90s, the technique for precise measurement of Mg/Ca composition of biogenic carbonates from oceanic sediments was developed<sup>12,13</sup>. The incorporation of Mg in biogenic carbonates varies with the changes in ambient seawater temperature<sup>14</sup>. Thus the Mg/Ca ratio of the biogenic carbonates helps to generate more precise SST records from different parts of the world oceans. Additionally, though the processing procedure is tedious<sup>10</sup>, the reproducibility of the results is good and the estimated seawater temperatures are precise. By using this technique, it is further possible to estimate seawater temperature at different depths of the water column, by using planktic foraminiferal species that live at different depths in the water column.

Here, SST records covering the last 150 kyr, from the equatorial Pacific, Indian and Atlantic Oceans<sup>15–21</sup> have been compiled. This time interval was chosen as it covers the two time periods of particular interest as mentioned above (LGM and last interglacial). However, in order to maintain the consistency in the data-sets, only those past SST records have been considered that are based on Mg/Ca analysis of the surface-dwelling planktic foraminifera *Globigerniodes ruber*.

Foraminifera are unicellular, preferentially marine microorganisms with their soft part encased in a hard outer skeleton or shell, technically called as test. The shell is generally calcareous but may also comprise sand particles cemented together. The calcareous tests also have minor amount of various elements (Mg, Cd, Ba, etc.) that replace the major elements (Ca) constituting the tests. The replacement of the major constituent elements of the test by other elements mainly depends on the chemical feasibility (size, valency and electronic configuration of the elements). Although possible physico-chemical control on the replacement of certain elements was suggested, complete understanding of the factors influencing the replacement of elements in the tests remained obscure for long due to inefficient cleaning procedures and non-availability of instruments to measure very low concentration of the elements. With the development of refined cleaning procedures<sup>22</sup> and measurement<sup>23</sup>, the application of various elemental ratios of foraminiferal tests emerged as efficient tool for paleoclimatic studies<sup>24</sup>.

The incorporation of Mg into the calcite is suggested to be temperature dependent<sup>25,26</sup> with a sensitivity of 3% increase in the Mg uptake for every 1°C rise in tempera-

ture, in case of inorganically precipitated calcite<sup>27</sup>. The temperature sensitivity of Mg uptake in foraminiferal calcite is reported to be of the order of 10% increase per 1°C increase of temperature<sup>28</sup>. The advantage of Mg/Ca paleothermometry lies in the long residence time of both Mg and Ca ( $10^7$  and  $10^6$  years respectively) and thus an almost constant Mg/Ca ratio of seawater over glacial–interglacial periods. However, the Mg–Ca content of foraminiferal tests is altered by post-depositional dissolution of the foraminiferal tests<sup>29</sup> for which measures have been suggested to estimate temperature, after correcting for dissolution-induced changes<sup>30</sup>. The pH and salinity of the seawater also affect the Mg/Ca ratio of the foraminiferal shells, but the changes are relatively small (–6% change in Mg/Ca for 0.1 pH unit increase and +4% per salinity unit increase)<sup>28,31</sup>. Based on various calibrations<sup>28,32,33</sup>, the seawater temperature can be calculated from the Mg/Ca ratio in foraminiferal calcite by using an equation of the following order

$$\text{Mg/Ca} = B \exp(A \times T),$$

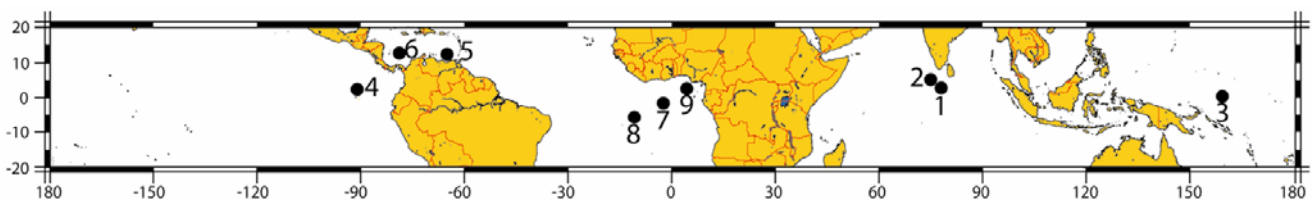
where  $A$  and  $B$  are species specific constants and  $T$  is temperature in °C.

Table 1 shows the details of the core site for which *G. ruber* Mg/Ca SST estimates are available and are used. The SST data of the selected cores was either downloaded from various websites or provided by the authors. Since the cores were collected from depths ranging from 790 to 3500 m, with varying distance from the nearby landmass (Figure 1), I have not emphasized much on SST at particular points in each core. Rather, the average SST during different marine isotopic stages (alternate cold and warm periods during the Quaternary that are related to the changes in the global ice-volume extent and are delineated on the basis of significant change in stable oxygen isotopic ratio of marine biogenic carbonates, especially foraminiferal shells; the cold periods are denoted by even numbers, whereas the odd numbers indicate warm periods; MIS 1–MIS 5), covering the last 150,000 years was calculated. Since MIS 5 covers both cold and warm periods, SST during MIS 5 was averaged over various sub-stages (MIS 5.1–MIS 5.5). The boundaries of the marine isotopic stages as defined by Bassinot *et al.*<sup>34</sup> are used. To compare the changes in SST during the past 150,000 years with respect to the modern, the January and July SSTs, and the annual SST of the equatorial region, are also given (Figure 2). Here it should be noted that the development of the chronology of the cores using different reservoir age correction, and calibration curves may slightly bias the results. Averaging SST for marine isotopic stages, however will help reduce this bias.

The foraminiferal Mg/Ca-based SST obtained from the core tops, matches well with the modern SST in all the records and the deviation is within the error limits (Table 1). It shows that the foraminiferal Mg/Ca ratio is an

**Table 1.** Details of the studied cores and Mg/Ca SST changes over Holocene–LGM interval. For assessing the reliability of the Mg/Ca SST, the modern climatological SSTs and core-top Mg/Ca SSTs are also given. The last column shows highest SSTs during the marine isotopic stage 5e. The core numbers are same as that given in location map (Figure 1)

Sl. no. (as in Figure 1)	Core number	Region	Ocean	Latitude	Longitude	Depth (m)	Refer- ence	Modern SST (°C)	Core top SST (°C)	$\Delta$ Holocene LGM SST (°C)	Peak MIS 5e SST (°C)
1	SK 157-04 (CEI 1)	Comorin Ridge	Cent. Indian	02.0°40.00'N	78.0°00.00'E	3500	15	28.5	28.1	-1.1	30.0 (123.0)
2	MD90-0963 (CEI 2)	Maldive Platform	Cent. Indian	05.0°04.00'N	74.0°53.00'E	2446	16	28.7	28.5	-2.6	29.8 (123.6)
3	ODP Hole 806B (WEP)	Ontong Java Plateau	West Pacific	00.0°19.10'N	159.0°21.70'E	2520	17	29.2	28.6	-2.7	29.6 (123.4)
4	TR163-19 (EEP)	Cocos Ridge	East Pacific	02.0°16.90'N	90.0°57.90'W	2348	17	26.2	25.8	-2.7	28.2 (122.0)
5	PL07-39PC (WEA 1)	Cariaco Basin	West Atlantic	10.0°42.00'N	64.0°56.50'W	790	18	26.0	26.9	-2.8	–
6	ODP999A (WEA 2)	Colombian Basin	West Atlantic	12.0°45.00'N	78.0°44.00'W	2827	19	27.7	28.2	-2.1	29.6 (128.6)
7	GeoB 1105-3/4 (EEA 1)	Guinea Basin	East Atlantic	01.0°39.90'S	12.0°25.70'W	3225	20	26.2– 22.3	24.7	-1.9	26.6 (122.0)
8	GeoB 1112-3/4 (EEA 2)	Guinea Basin	East Atlantic	05.0°46.20'S	10.0°44.70'W	3122	20	25.5– 23.3	26.1	-2.3	27.6 (121.5)
9	MD03-2707 (EEA 3)	Gulf of Guinea	East Atlantic	02.0°30.11'N	09.0°23.68'E	1295	21	–	25.3	-2.7	28.3 (124.5)



**Figure 1.** Core locations in the equatorial ocean, whose data is used for this work. 1, Saraswat *et al.*<sup>15</sup>; 2, Tachikawa *et al.*<sup>16</sup>; 3, 4, Lea *et al.*<sup>17</sup>; 5, Lea *et al.*<sup>18</sup>; 6, Schmidt *et al.*<sup>19</sup>; 7, 8, Nuernberg *et al.*<sup>20</sup>; 9, Weldeab *et al.*<sup>21</sup>.

efficient proxy to estimate seawater temperature. The maximum SST change over the last 150,000 years is recorded in the eastern equatorial Atlantic Ocean (6.5°C) whereas the minimum is in the western equatorial Pacific Ocean (3.7°C; Figure 3). The range of change in SST over the last 150 kyr is same at one location in the western equatorial Atlantic Ocean and the eastern equatorial Pacific Ocean (5.9°C). However, here I would like to emphasize that part of the range of these SST variations in different equatorial regions over the last 150 kyr is due to the difference in the distance of the core locations from the adjacent coastline as well as the unique seawater circulation features. The distance of the location from the land is an important factor as several near shore regions are affected by coastal upwelling, which brings in nutrient rich cold deep water to the surface, thus altering the effect of insolation<sup>35</sup>. The fresh water runoff by large rivers draining from the nearby landmass, can also affect SST<sup>36</sup>. Additionally, coastal currents also affect the seawater temperature in the near-shore regions as these cur-

rents transport significant amount of water from one basin to another<sup>37</sup>. In contrast to that, seawater temperature at the open ocean locations, is mainly controlled by the solar insolation changes.

The period from 23 to 19 kyr BP is considered as the LGM after MARGO<sup>8</sup>. The Mg/Ca SST estimates indicate that the surface equatorial oceans were ~2.3°C cooler during LGM, as compared to the Holocene. The LGM–Holocene SST difference varies from 1.1°C to 2.8°C, which implies that seawater temperature gradient in the equatorial oceans during LGM was not the same as that of the present. Different hydrological regimes at core locations, as mentioned before, may result in differential cooling during LGM. But, ~2.5°C cooling during LGM as compared to the Holocene, is recorded in majority of the records (six out of nine). Less than 2.0°C cooling during Holocene–LGM transition is observed in the Indian Ocean (SK157-04) and the eastern Atlantic Ocean (ODP999A). A few other studies which used Mg/Ca in *G. ruber* to estimate SST in the tropical and equatorial

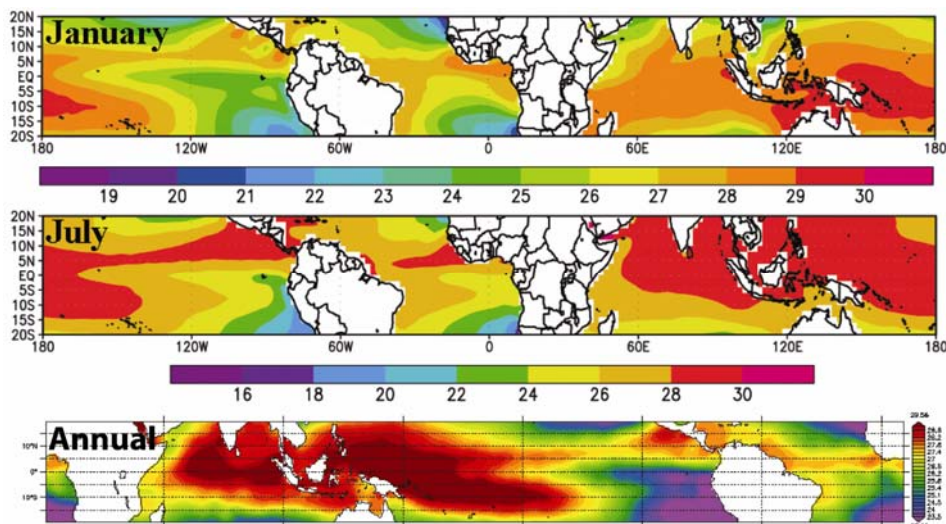


**Figure 2.** Sea-surface temperature (SST) in the equatorial region during January and July. The annual average SST of the equatorial regions is also given.

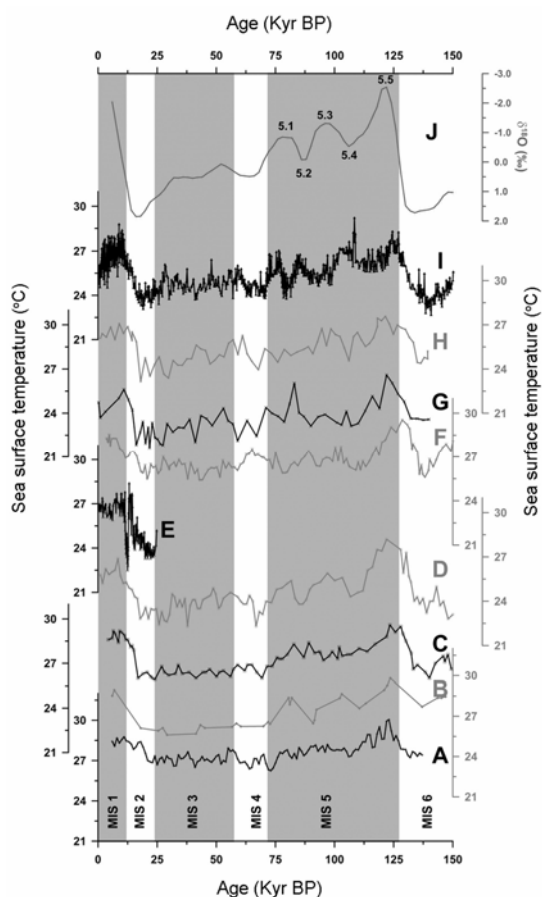


**Figure 3.** Mg/Ca SST variation in studied cores over the last 150,000 years. A, Central Equatorial Indian Ocean<sup>15</sup>; B, Central Equatorial Indian Ocean<sup>16</sup>; C and D, Western and Eastern Equatorial Pacific Ocean<sup>17</sup>; E, Western Equatorial Atlantic Ocean<sup>18</sup>; F, Western Equatorial Atlantic Ocean<sup>19</sup>; G, H, Eastern Equatorial Atlantic Ocean<sup>20</sup>; I, Eastern Equatorial Atlantic Ocean<sup>21</sup>. To understand the duration of different marine isotopic stages, global oxygen isotopic stack of Bassinot *et al.*<sup>34</sup> has also been plotted as reference curve (J). Alternate grey bands indicate alternate marine isotopic stages. Different marine isotopic stages (MIS) are also marked. Different sub-stages during MIS 5 are marked by numbers in the global oxygen isotopic stack.

Indian Ocean during LGM, indicate 3–4°C drop in SST<sup>38,39</sup>. These studies were however carried out from regions affected by seasonally reversing monsoon currents and upwelling. Studies that used alkenone unsaturation index to estimate SST, indicate ~1.7°C change in SST during LGM–Holocene transition, in the equatorial-tropical Indian Ocean<sup>40</sup>. It should however be noted that recently, it was observed that alkenone unsaturation index may not indicate annual SST possibly due to the change in species that contributes maximum alkenone, lateral transport of alkenone-bearing material and/or a change in depth distribution of alkenone producing species<sup>41</sup>. The Mg/Ca-based estimates of drop in SST in the Indian Ocean during LGM also match well with the modern analogue technique-based LGM SST cooling estimates<sup>11</sup>. The same study however showed 5–7°C LGM cooling at several locations in the eastern equatorial Atlantic which is significantly higher (almost two times higher) than Mg/Ca-based LGM cooling estimates for this region. The Mg/Ca-based estimates of drop in SST during LGM are also contradictory to the findings of the MARGO project, wherein generally larger cooling was reported in the Atlantic Ocean<sup>8</sup>. Similarly, Mg/Ca estimates of glacial cooling in the eastern Atlantic are also much lower than the results of Maximum Similarity Technique Version 28 (SIMMAX-28) modern analogue technique wherein it was inferred that LGM SST in the tropical east Atlantic upwelling region was 6–8°C cooler during northern hemisphere summer<sup>10</sup>. However, the present findings are based on a few records.

As compared to MIS 2, SST during MIS 3 was either similar or slightly colder (Figure 4). SST during MIS 4 was also as cold as that during MIS 3 or MIS 2, at most of the locations (except at one location each in eastern and western equatorial Atlantic Ocean). However, a few other studies show that SST during MIS 4 was higher



than that during MIS 3 in the upwelling region of the tropical eastern Arabian Sea<sup>39</sup>.

The Mg/Ca estimated SST during MIS 5.5 is warmest of the entire last 150 kyr, also higher (1–2°C warmer) than that during the Holocene (Table 1, Figure 4). It shows that between 127,000 and 122,000 years BP when there was no anthropogenic influence, the surface seawaters in the equatorial regions were warmer than that at present. It should however be kept in mind that this warming was also accompanied by a concomitant increase in atmospheric CO<sub>2</sub> concentration as estimated from ice core records<sup>42</sup>. It implies that temperature changes on earth are possibly related to the changes in atmospheric CO<sub>2</sub> concentration. The atmospheric CO<sub>2</sub> concentration during MIS 5.5 was comparable with the preindustrial atmospheric CO<sub>2</sub> concentration during the Holocene. A substantial cooling (as compared to MIS 5.5) is reported during MIS 5.4, all throughout the equatorial oceans, except in the eastern equatorial Atlantic Ocean (Figure 4). However, insignificant drop in surface seawater temperature is observed between MIS 5.5 and MIS 5.3, at two sites in the eastern equatorial Atlantic Ocean (Figure 4). The equatorial ocean SST continued to drop even during MIS 5.3, except in the central equatorial Indian Ocean, wherein seawater during MIS 5.3 was warmer than that during MIS 5.4. The surface equatorial oceans during MIS 5.3 were warmer than that during MIS 5.1 at all the sites except in the eastern equatorial Atlantic ocean. The SST further dropped during MIS 5.2, with most extensive decline noted at one site in the equatorial Indian Ocean. Substantial warming during MIS 5.2–MIS 5.1 transition was observed only at two sites, one each in equatorial Indian and eastern equatorial Atlantic Oceans (Figure 4). At rest of the places, surface seawater continued to drop even during MIS 5.1. The study shows that the surface equatorial oceans were not necessarily cold and warm during alternate marine isotopic stages and sub-stages as

inferred from changes in stable oxygen isotopic ratio ( $\delta^{18}\text{O}$ ) of marine biogenic carbonates. The variation in  $\delta^{18}\text{O}$ , which is used to mark cold (enriched  $\delta^{18}\text{O}$ ) and warm (depleted  $\delta^{18}\text{O}$ ) periods, may indicate changing ice-sheet extent. Different physiographic conditions, especially the current direction and upwelling are probably responsible for the differential response of various parts of equatorial oceans during various sub-stages of MIS 5. It was however, difficult to assess SST during marine isotopic stage 6, as a few of the records do not cover the total 150,000 years BP.

This reanalysis of the Mg/Ca SST changes from the global equatorial oceans covering the last 150 kyr shows that:

- The average cooling during LGM was ~2.3°C as compared to the Holocene. The surface equatorial temperature gradient during LGM was different from that at present.
- The equatorial surface waters were warmest during the MIS 5.5, even warmer than that at present.
- The pattern of cooling and amount of drop in surface temperature during MIS 5 was not uniform throughout the equatorial oceans.
- Several regions of the surface equatorial oceans during MIS 4 were warmer than that during MIS 3.
- The study further shows that surface equatorial oceans during MIS 3 were as cold as during MIS 2.

The consistency of Holocene–LGM SST differences, as well as the similar general patterns of cooling and warming during various marine isotopic stages at most of the sites reinforce the robustness of Mg/Ca-based SST estimates.

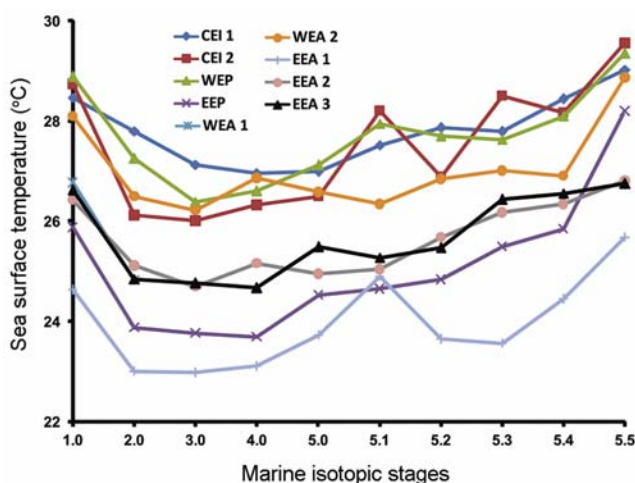


**Figure 4.** Mg/Ca SST variation during different marine isotopic stages. For details of the core sites, refer Table 1.

1. Broecker, W., *The Great Ocean Conveyor: Discovering the Trigger for Abrupt Climate Change*, Princeton University Press, 2010, p. 172.
2. Gadgil, S., The Indian monsoon and its variability. *Annu. Rev. Earth Planet. Sci.*, 2003, **31**, 429–467.
3. CLIMAP Project Members, The surface of the ice-age Earth. *Science*, 1976, **191**, 1131–1137.
4. CLIMAP Project Members, Seasonal reconstructions of the Earth's surface at the last glacial maximum. Geological Society of America Map and Chart Series, MC-36, Geological Society of America, Boulder, CO, 1981.
5. Hoffert, M. I. and Covey, C., Deriving global climate sensitivity from paleoclimate reconstructions. *Nature*, 1992, **360**, 573–576.
6. Chen, M.-T., Huang, C.-C., Pflaumann, U., Waelbroeck, C. and Kucera, M., Estimating glacial western Pacific sea-surface temperature: methodological overview and data compilation of surface sediment planktic foraminifer faunas. *Quat. Sci. Rev.*, 2005, **24**, 1049–1062.
7. Gates, W. L., Modeling the ice-age climate. *Science*, 1976, **191**, 1138–1144.
8. MARGO Project Members, Constraints on the magnitude and patterns of ocean cooling at the Last Glacial Maximum. *Nat. Geosci.*, 2009.

9. Rosell-Mele, A., Bard, E., Emeis, K. C., Grieger, B., Hewitt, C., Muller, P. J. and Schneider, R. R., Sea surface temperature anomalies in the oceans at the LGM estimated from the alkenone-UK' 37 index: comparison with GCMs. *Geophys. Res. Lett.*, 2004, **31**, L03208.
10. Pflaumann, U. *et al.*, Glacial North Atlantic: Sea-surface conditions reconstructed by GLAMAP 2000. *Paleoceanography*, 2003, **18**, 1065.
11. Trend-Staid, M. and Prell, W. L., Sea surface temperature at the last glacial maximum: a reconstruction using the modern analog technique. *Paleoceanography*, 2002, **17**.
12. Nuernberg, D., Bijma, J. and Hemleben, C., Assessing the reliability of magnesium in foraminiferal calcite as a proxy for water mass temperatures. *Geochim. Cosmochim. Acta*, 1996, **60**, 803–814.
13. Lea, D. W., Mashiotta, T. A. and Spero, H. J., Controls on magnesium and strontium uptake in planktonic foraminifera determined by live culturing. *Geochim. Cosmochim. Acta*, 1999, **63**, 2369–2379.
14. Chave, K. E., Aspects of the biogeochemistry of magnesium 1. Calcareous marine organisms. *J. Geol.*, 1954, **62**, 266–283.
15. Saraswat, R., Nigam, R., Weldeab, S., Mackensen, A. and Naidu, P. D., A first look at past sea surface temperatures in the equatorial Indian Ocean from Mg/Ca in foraminifera. *Geophys. Res. Lett.*, 2005, **32**, L24605.
16. Tachikawa, K., Se'pulcre, S., Toyofuku, T. and Bard, E., Assessing influence of diagenetic carbonate dissolution on planktonic foraminiferal Mg/Ca in the southeastern Arabian Sea over the past 450 ka: comparison between *Globigerinoides ruber* and *Globigerinoides sacculifer*. *Geochem. Geophys. Geosyst.*, 2008, **9**, Q04037.
17. Lea, D. W., Pak, D. K. and Spero, H. J., Climate impact of late Quaternary equatorial Pacific sea surface temperature variations. *Science*, 2000, **289**, 1719–1724.
18. Lea, D. W., Pak, D. K., Peterson, L. C. and Hughen, K. A., Synchronicity of tropical and high-latitude Atlantic temperatures over the last glacial termination. *Science*, 2003, **301**, 1361–1364.
19. Schmidt, M. W., Vautravers, M. J. and Spero, H. J., Western Caribbean Sea surface temperatures during the late Quaternary. *Geochem. Geophys. Geosyst.*, 2006, **7**, Q02P10.
20. Nuernberg, D., Miiller, A. and Schneider, R. R., Paleo-sea surface temperature calculations in the equatorial east Atlantic from Mg/Ca ratios in planktic foraminifera: A comparison to sea surface temperature estimates from  $U_{37}^K$ , oxygen isotopes, and foraminiferal transfer function. *Paleoceanography*, 2000, **15**, 124–134.
21. Weldeab, S., Lea, D. W., Schneider, R. R. and Andersen, N., 155,000 years of West African monsoon and ocean thermal evolution. *Science*, 2007, **316**, 1303–1307.
22. Barker, S., Greaves, M. and Elderfield, H., A study of cleaning procedures used for foraminiferal Mg/Ca paleothermometry. *Geochem. Geophys. Geosyst.*, 2003, **4**, 8407.
23. Shen, C.-C. *et al.*, High precision measurements of Mg/Ca and Sr/Ca ratios in carbonates by cold plasma inductively coupled plasma quadrupole mass spectrometry. *Chem. Geol.*, 2007, **236**, 339–349.
24. Barker, S., Cacho, I., Benway, H. and Tachikawa, K., Planktonic foraminiferal Mg/Ca as a proxy for past oceanic temperatures: a methodological overview and data compilation for the Last Glacial Maximum. *Quat. Sci. Rev.*, 2005, **24**, 821–834.
25. Chave, K. E., Aspects of the biogeochemistry of magnesium 1. Calcareous marine organisms. *J. Geol.*, 1954, **62**, 266–283.
26. Oomori, T., Kaneshima, H. and Maezato, Y., Distribution coefficient of  $Mg^{2+}$  ions between calcite and solution at 10–50°C. *Mar. Chem.*, 1987, **20**, 327–336.
27. Rosenthal, Y., Boyle, E. A. and Slowey, N., Temperature control on the incorporation of magnesium, strontium, fluorine, and cadmium into benthic foraminiferal shells from Little Bahama Bank: Prospects for thermocline paleoceanography. *Geochim. Cosmochim. Acta*, 1997, **61**, 3633–3643.
28. Lea, D. W., Mashiotta, T. A. and Spero, H. J., Controls on magnesium and strontium uptake in planktonic foraminifera determined by live culturing. *Geochim. Cosmochim. Acta*, 1999, **63**, 2369–2379.
29. Brown, S. J. and Elderfield, H., Variations in Mg/Ca and Sr/Ca ratios of planktonic foraminifera caused by postdepositional dissolution: Evidence of shallow Mg-dependent dissolution. *Paleoceanography*, 1996, **11**, 543–551.
30. Rosenthal, Y. and Lohmann, G. P., Accurate estimation of sea surface temperatures using dissolution-corrected calibrations for Mg/Ca paleothermometry. *Paleoceanography*, 2002, **17**, 1044.
31. Dissard, D., Nehrke, G., Reichart, G. J. and Bijma, J., The impact of salinity on the Mg/Ca and Sr/Ca ratio in the benthic foraminifera *Ammonia tepida*: results from culture experiments. *Geochim. Cosmochim. Acta*, 2010, **74**, 928–940.
32. Dekens, P. S., Lea, D. W., Pak, D. K. and Spero, H. J., Core top calibration of Mg/Ca in tropical foraminifera: refining paleotemperature estimation. *Geochem. Geophys. Geosyst.*, 2002, **3**, 1022.
33. Anand, P., Elderfield, H. and Conte, M. H., Calibration of Mg/Ca thermometry in planktonic foraminifera from a sediment trap time series. *Paleoceanography*, 2003, **18**, 1050.
34. Bassinot, F. C., Labeyrie, L. D., Vincent, E., Quidelleur, X., Shackleton, N. J. and Lancelot, Y., The astronomical theory of climate and the age of the Brunhes-Matuyama magnetic reversal. *Earth Planet. Sci. Lett.*, 1994, **126**, 91–108.
35. Shi, W., Morrison, J. M., Böhm, E. and Manghnani, V., The Oman upwelling zone during 1993, 1994 and 1995. *Deep Sea Res. II: Topical Studies Oceanogr.*, 2000, **47**, 1227–1247.
36. Howden, S. D. and Murtugudde, R., Effects of river inputs into the Bay of Bengal. *J. Geophys. Res.*, 2001, **106**, 19825–19843.
37. Shankar, D., Vinayachandran, P. N. and Unnikrishnan, A. S., The monsoon currents in the north Indian Ocean. *Progr. Oceanogr.*, 2002, **52**, 63–120.
38. Anand, P., Kroon, D., Singh, A. D., Ganeshram, R. S., Ganssen, G. and Elderfield, H., Coupled sea surface temperature–seawater  $\delta^{18}O$  reconstructions in the Arabian Sea at the millennial scale for the last 35 ka. *Paleoceanography*, 2008, **23**, PA4207.
39. Govil, P. and Naidu, P. D., Evaporation–precipitation changes in the eastern Arabian Sea for the last 68 ka: implications on monsoon variability. *Paleoceanography*, 2010, **25**, PA1210.
40. Bard, E., Rostek, F. and Sonzogni, C., Interhemispheric synchrony of the last deglaciation inferred from alkenone paleothermometry. *Nature*, 1997, **385**, 707–710.
41. Saher, M. H. *et al.*, Western Arabian Sea SST during the penultimate interglacial: a comparison of  $U_{37}^K$  and Mg/Ca paleothermometry. *Paleoceanography*, 2009, **24**, PA2212.
42. Fischer, H., Wahlen, M., Smith, J., Mastoianni, D. and Deck, B., Ice core records of atmospheric  $CO_2$  around the last three glacial terminations. *Science*, 1999, **283**, 1712–1714.

ACKNOWLEDGEMENTS. I thank Dr R. Nigam of the National Institute of Oceanography, Goa for the encouragement to publish the findings and Dr V. K. Banakar in improving an earlier version of this manuscript. I also thank the anonymous reviewer for constructive comments and suggestions which helped improve the manuscript.

Received 6 August 2010; revised accepted 14 January 2011